Generalizable Neural Models of Emotional Engagement and Disengagement

Melanni Nanni-Zepeda[1,2], Travis C. Evans[13,15], Audreyana Jagger-Rickels[12,14,16], Gal Raz[3,4,5], Talma Hendler[4,5,6,7], Yan Fan[8], Simone Grimm[9,10,11], Martin Walter[1,2,16,17], Michael Esterman[12, 15], and Agnieszka Zuberer[1,2,18,19]

[1]Department of Psychiatry and Psychotherapy, Jena University Hospital, 07743 Jena, Germany

[2]Department of Psychiatry and Psychotherapy, University of Tübingen, 72076 Tübingen, Germany

[3]Steve Tisch School of Film and Television, Tel Aviv University, Tel Aviv, Israel

[4]Sagol School of Neuroscience, Tel Aviv University, Tel Aviv, Israel

[5]Sagol Brain Institute, Tel Aviv Sourasky Medical Center, Tel Aviv, Israel

[6]Sackler Faculty of Medicine, Tel Aviv University, Tel Aviv, Israel

[7]The School of Psychological Sciences, Tel Aviv University, Tel Aviv, Israel

[8]Department Psychology and Neurosciences, Leibniz Research Centre for Working Environment and Human Factors at the TU Dortmund (IfADo), Dortmund, Germany

[9]Department of Psychiatry, Psychotherapy and Psychosomatics, Psychiatric Hospital, University of Zurich, Zurich, Switzerland

[10]Department of Psychology, MSB Medical School Berlin, Berlin, Germany

[11]Berlin Institute of Health, Campus Benjamin Franklin, Charité-Universitätsmedizin Berlin, Corporate Member of Freie Universität Berlin, Humboldt-Universität zu Berlin,

Berlin, Germany

[12]National Center for PTSD, VA Boston Healthcare System, Boston, MA, USA

[13]Boston Attention and Learning Laboratory, VA Boston Healthcare System, Boston, MA, 02130, USA

[14]Department of Psychiatry, Harvard Medical School, Boston, MA, USA

[15]Department of Psychiatry, Boston University Chobanian and Avedisian School of Medicine, Boston, MA, USA

[16]Center for Intervention and Research on adaptive and maladaptive brain Circuits underlying mental health (C-I-R-C), Halle-Jena-Magdeburg, Germany

[17]German Center for Mental Health (DZPG), partner site Halle-Jena-Magdeburg, Germany

[18]Department of Psychiatry, University of North Carolina, Chapel Hill, NC 27599, USA

[19]Carolina Center for Neurostimulation, University of North Carolina, Chapel Hill, NC 27599, USA

Author Note

Correspondence concerning this article should be addressed to Melanni Nanni-Zepeda, Department of Psychiatry and Psychotherapy, Attention and Affect Laboratory, Eberhard Karls University, Tübingen, Germany. E-mail: nanni.melanni@gmail.com and azuberer@gmail.com

Abstract

Emotional reactivity to negative content profoundly impacts our mental well-being and is a hallmark of disorders characterized by emotion dysregulation. Traditional approaches have examined emotional responses and regulation in isolation, neglecting their temporal dynamics. Movie designs can capture both, in their natural progression throughout time, yet they pose complexity due to the mix of relevant and irrelevant information. To address these challenges and uncover general neural mechanisms of affect, we used dynamic predictive modeling across different narratives, emotional contexts, and participant groups. We analyzed two independent data sets containing different narratives of highly emotionally negative content and one neutral narrative during functional magnetic resonance imaging (fMRI). Following fMRI scanning, individuals provided continuous subjective annotations of emotional intensity throughout these movie clips. Patterns of dynamic functional connectivity predicting group response of emotional disengagement in negative movies generalized to diverse narratives and participants, demonstrating specificity to negative content. This prediction involved widespread between-network connections increases. Conversely, emotional engagement generalized across narratives and participants, including neutral contexts, with a less intense emotional intensity induction. Prediction for engagement was marked by widespread between-network connections decreases. Activation analyses distinguished brain regions for disengagement in the default network and engagement in the dorsal attention and visual network. These patterns remained consistent across studies and emotional contexts, revealing generic engagement and disengagement responses even in less emotional movie contexts. These findings demonstrate that movies elicit behavioral and neural responses that contribute to understanding the ecological generalizability of emotional cinematic experiences. Together this work helps to better understand cognitive and neural mechanisms underpinning engagement *in* and disengagement *from* emotionally evocative narratives.

Keywords: movie, emotion, emotional intensity, engagement, disengagement, fMRI

Generalizable Neural Models of Emotional Engagement and Disengagement

Significance statement:

How emotions unfold over time has been a subject of significant theoretical debate. In real life, negative emotional reactions often trigger a subsequent phase of regulation aimed at returning to a state of emotional equilibrium. However, the neural processes underlying these phases are rarely studied in their natural temporal progression. Functional MRI experiments using movies offer an opportunity to simulate these real-life scenarios, enabling individuals to empathize with characters and immerse themselves in hypothetical real-life situations. These experiments have revealed that emotional responses to negative movie content, along with the regulation of these responses, lead to significant reorganizations in the brain's architecture. Notably, these reorganizations differ when individuals react emotionally compared to when the emotional experience wanes.

Introduction

Our well-being profoundly depends on the way we engage *in* and disengage *from* emotions when interacting with others and the world. Theories of affect have widely acknowledged that there is a temporal progression of an emotional response and its regulation (e.g. Gross et al. (2014); Scherer (2009); Sheppes and Gross (2011)pp. 16-17). However, empirically the neural mechanisms underlying these processes have traditionally been studied in isolation, disregarding their dynamic nature throughout time. In real life, emotions evolve temporally, and naturalistic scenarios like movies have been shown to mirror this phenomenon. Movies evoke a rich dynamic affective experience (Morgenroth et al., 2022; Saarimäki, 2021; Sonkusare et al., 2019). This experience involves periods of both engagement and disengagement, mirroring the natural fluctuations that occur over time. However, when gauging emotional responses through movies, there is a diverse range of movie-related content, each contributing differently to the overall emotional experience. For instance, involvement in sad emotions could be induced by an emotionally charged dialogue where the protagonist discovers the loss of a significant other. In contrast factors such as the color of the actor's costumes, people passing by in the background, the camera perspective, or the sentence structure might have little relevance to the emotional experience. Although movies have the potential to mimic real-life scenarios, there is a challenge for affective movie fMRI in terms of ecological validity not necessarily directly translating to ecological generalizability. This implies that the findings may not extend uniformly across various naturalistic contexts (Nastase et al., 2020). Predictive modeling of a dynamic affective experience across various movies and participant groups holds the potential to unveil more generalized neural mechanisms relevant to the actual emotional experience, independent from the idiosyncratic nature of each movie. This way, common patterns and neural responses can be distilled that transcend specific cinematic content and individual differences. In the limited scope of fMRI studies employing dynamic predictive modeling to assess neural mechanisms underlying affect and attention, findings indicate a central role for the default mode network (DMN). For instance, in a study using short (1-minute) audio narratives one study was able to predict 6 emotions of interest based on within-DMN connectivity (Saarimäki et al., 2022). Further, DMN connectivity was predictive of attentional engagement in a narrative across a movie and audiobook (Song et al., 2021). This suggests that the DMN may serve as a key hub in processing and predicting emotional experiences during naturalistic stimuli involving narratives. In a separate study, researchers achieved the prediction of dynamic fear responses across both an entire fearful movie and a short movie excerpt (Zhou et al., 2023). This was accomplished by leveraging redundant widespread large-scale brain network connectivity, without relying on specific network subsystems. These findings suggest that a broader network perspective, encompassing various interconnected brain regions, can contribute to the predictive modeling of dynamic emotional responses during exposure to fear-inducing stimuli in the cinematic context. Together this work establishes a foundation for linking brain activity with varying levels of subjective attention or affect. Nonetheless, there is still a significant gap in our understanding of the neural mechanisms that initiate shifts in the subjective emotional experience. Here, we aim to assess the mechanisms involved in two transitional stages of dynamic adaptation to emotional stimuli, specifically focusing on when individuals recognize and respond to an incremental shift in emotional intensity and the subsequent shift towards a decrease in intensity. The incremental transitional stage draws audiences deeper into the narrative with each nuanced shift. Throughout this dynamic progression, viewers become immersed in the nuanced shifts of emotional intensity, fostering a more profound connection with the narrative. The emphasis is on the shifts rather than distinct peaks, as viewers steadily navigate the evolving emotional landscape. The subsequent phase, marked by a shift towards a decrease of emotional intensity involves a winding down of the emotional journey. As the emotional journey recedes, viewers process the preceding intense emotional experience, e.g. through regulation strategies such as cognitive re-appraisal or expressive suppression (Koval, Butler, et al., 2015; Kuppens & Verduyn, 2015). The dynamics of these alternations play a pivotal role in shaping the emotional experience itself: the manner in which we engage in an emotion influences subsequent disengagement and, consequently, re-engagement in emotions (Koval, Brose, et al., 2015). Thus, it is critical to elucidate the temporal dynamics of engagement and disengagement as they naturally evolve throughout time, along with their corresponding neural signatures.

To achieve this objective, we employed two independent datasets, where participants retrospectively provided subjective emotional intensity annotations in response to either one negative and one neutral movie clip (Study 1) or one negative movie clip (Study 2) during functional magnetic resonance imaging (fMRI) scanning. Within the temporal fluctuations of individual annotations of affect, we identified moments of positive and negative shifts of subjective emotional intensity, here called emotional engagement (EE) and disengagement (ED). Our initial inquiry was to assess dynamic functional connectivity patterns supporting collective group changes of EE and ED patterns throughout movie viewing. To this aim, we used support vector regression (SVR) to predict EE and ED across independent participant groups, movie clips of either high or low emotional intensity. Our second objective was to pinpoint brain activation patterns time-locked to moments of EE and ED. We achieved this by analyzing lower-dimensional group features of the affective experience through principal component analysis. Based on the evidence described above, we expected that both within-DMN connectivity specifically and large-scale network connectivity more generally could play a central role in predicting EE and ED. We additionally hypothesized that brain regions belonging to the dorsal, ventral attention and visual systems could potentially support EE, while DMN and central executive network (CEN) would support ED. However, given the lack of predictive studies of affect in naturalistic scenarios, we did not constrain our analysis to specific regions of interest. In summary, our analysis demonstrated that patterns of functional connections, initially trained to predict ED in negative movies, effectively generalized to diverse narratives and participants, excluding neutral contexts. This indicates their specificity to high emotional intensity situations. Successful prediction in this context featured widespread increases in between-network connectivity. Conversely, models predicting EE successfully generalized across various scenarios, even in neutral contexts, suggesting no specificity to high emotional intensity. Accurate prediction of EE was marked by widespread decreases in between-network connections. Activation analyses revealed that

ED was linked to higher activations in the default network, while EE was linked to higher activations in the dorsal attention (DAN) and visual network. These activation patterns remained consistent across studies and emotional contexts, suggesting generic EE and ED signature responses even in less emotional movie contexts. To the best of our knowledge, this study marks the initial endeavor to differentiate the dynamic neural mechanisms underlying EE and ED during an emotional cinematic experience.

Results

Distinctive Patterns of Emotional Engagement and Disengagement

We analyzed both fMRI and behavioral data from two independent studies each employing similar paradigms and data acquisition methods. In Study 1, participants viewed 5-minute excerpts from two movies ("21 Grams" and "Son’s Room") in a counterbalanced order (Borchardt et al., 2018). The "21 Grams" clip depicts a mother discovering the death of her two daughters, while the "Son’s Room" clip shows scenes of the daily life of a family with casual chats and interactions (n=21; mean age 28.1 ∓ 6.5). Approximately 15 minutes after the scanning, participants rewatched both movie clips outside the scanner while providing continuous emotional intensity ratings concerning how they felt the first time they watched the movie. Subjects used a computer mouse to move a bar on a 250-point visual analog scale to annotate their emotional intensity (0=minimum, 250=maximum). This scale was adjacent to the video playback, allowing subjects to annotate and concurrently watch the video. In Study 2, participants watched an excerpt from the movie "Sophie’s Choice" depicting a mother confronted with the decision of selecting which of her children to rescue from death (n=42; mean age 26.73 ∓ 4.69); Raz et al., 2016. Similar to Study 1, subjective annotations were conducted outside of the scanner during the second movie watch using a 7-point Likert scale, where each of the seven points was subdivided into three sub-levels. Thus, the scale comprised 21 units to rate their momentary emotional intensity (0=minimum, 21=maximum). Subjects used a computer mouse to move the level of a bar either upward or downward to change the intensity from "neutral" to "very high". This retro-active annotating approach used in both studies is often chosen because real-time annotations during scanning modify neural responses to emotional stimulation, while repeated movie watching only minimally affects subjective annotations (Hutcherson et al., 2005; Lieberman et al., 2007). Time points of EE were identified as moments in time when subjective emotional intensity rose, reflected in a positive change between two consecutive points. Conversely, time points of ED were identified as moments in time when subjective emotional intensity decreased, reflected in a negative change between two consecutive points. Focusing on data between the 33rd and 67th percentiles enabled us to disregard extreme highs and lows. This algorithm used in previous studies to describe rises, decreases, peaks and troughs of neural responses (Dessu et al., 2020; Shine et al., 2019). This analysis resulted in two binary time courses for each subject, indicating whether a moment in time is labeled as EE (yes/no) or ED (yes/no).

In the negative clip of Study 1, participants reported an average of 6.90∓4.82 EE time points (4.9% ∓3.4%), and 2.40∓3.14 ED time points (1.7% ∓ 2.22%), with a mean duration of 13.81∓9.65 seconds for EE and 4.81∓6.28 seconds for ED. For the negative clip of Study 2, participants reported an average of 3.8∓2.46 EE time points (1.9% ∓1.23%) and 1.4∓1.42 ED time points (0.7% ∓ 0.71%), with a mean duration of 11.4∓7.39 seconds for EE and 4.2∓4.26 seconds for ED. In the neutral clip of Study 1, there were, on average, 1.31∓1.64 EE time points (0.9%∓1.12%) and 0.9∓1.63 ED phases (0.62%∓1.11%), with a mean duration of 2.63∓3.28 seconds for EE and 1.81∓3.26 seconds for ED. In each movie clip, some participants did not exhibit EE time points (3 subjects from the negative movie clip of Study 1 and 10 subjects from the neutral movie of Study 1), and some did not have ED time points (10 subjects from the negative movie clip of Study 1, 15 subjects from the negative movie clip of Study 2, and 13 subjects from the neutral movie clip of Study 2).

We expected that emotional movies would induce more emotional shifts (EE and ED) than the neutral clip. To test this, we built linear mixed-effects models by choosing a step-up approach (Hox et al., 2017) including an effect in the model if it significantly improved the model fit. A model fit was improved if the difference between the log-likelihood ratio of a model that contained the effect and a model that did not was significant (as compared with ANOVA; p<0.05). We used mixed effects modeling to test if the number of shifts could be predicted by emotional condition (negative/neutral) and emotional shift (EE/ED) with subjects as a random intercept, and movie duration as a fixed effect. The results revealed a significant interaction effect between emotional context and emotional shift (β = 1.18; 95% CI: [0.17, 2.18], $p = .02$). A post-hoc test revealed that (1) the number of emotional shifts was higher during the negative condition compared to neutral condition for both EE and ED (EE: estimate[neutral-negative]= -2.60; ∓0.411 95% CI: [-3.41, -1.79], $p < .001$; ED: estimate [neutral-negative]= -1.42; ∓0.486 95% CI: [-2.39, -0.46], $p = .004$); and (2) the number of EE was higher than ED in negative condition (estimate[ED -EE] = -1.68; ∓0.275; 95% CI: [-2.22, -1.13], $p < .001$) with no significant difference between EE and ED in the neutral condition (estimate[ED-EE]= -0.50; ∓0.428 95% CI: [-1.35, 0.34], $p = .244$)

In line with previous research demonstrating that emotion induction tends to induce some agreement between subjective affective responses (Li et al., 2015; Malandrakis et al., 2011), we initially explored whether our data showed a similar pattern and if so, whether the increased alignment was indeed owed to the higher emotional intensity in one clip as compared to the neutral one. Hence, we tested if (1) the ISC of emotional shifts was higher for emotional clips as compared to the neutral clip and (2) if ISC was different for EE and ED. To investigate this, we employed a mixed-effects model predicting ISC by the interaction of condition (negative/neutral) and emotional shift (EE and ED). The interaction effect was significant (β = -0.03; 95% CI: [-0.03, -0.02], $p < .001$). A post-hoc test revealed that ISC (1) was higher during emotionally intense as compared to neutral content for EE (estimate[neutral-negative]= -0.233 ∓0.001; 95% CI: [-0.237, -0.230], $p < .001$) and ED (estimate[ED-EE]= -0.262 ∓0.001; 95% CI: [-0.265, -0.258], $p < .001$) and (2) ISC was higher for ED as compared to EE in the negative condition (estimate[ED-EE]= 0.26 ∓0.001; 95% CI: [0.024, 0.027], $p < .001$). There was no significant difference between ISC for EE and ED in the neutral condition (estimate[ED-EE]= -0.002 ∓0.002; 95% CI: [-0.006, 0.001], $p = .279$). Together these findings suggest that emotionally intense negative movie material (1) aligns subjective emotional responses and (2) is enhanced for ED patterns as compared to EE patterns and (3) neither of the two are influenced by the degree to which subjects resemble in the overall number of emotional shifts. We further tested if the degree to which subjects align is influenced by how similar they are with each other in terms of the number of shifts. This was calculated by the normalized difference between subject scores, with normalization performed relative to the maximum absolute difference between subject scores. The inclusion of this similarity score did not improve the model fit, neither as 1) an additive effect, 2) interaction with either emotion condition or movie clip, nor 3) an interaction with both movie clip and shift type.

We then built a mixed-effects model to predict ISC of subjective emotional intensity by the interaction between the factors movie clip (21 grams, Son's room, Sophie's Choice) and emotional shift direction (EE/ED). This interaction effect between movie clip and emotional shift direction was significant ($\beta = 0.03$; 95% CI: [0.03, 0.04], $p < .001$). A post-hoc test revealed that ISC of EE was significantly different from ED in negative movie of Study 1 (estimate[ED-EE]= 0.051 ∓0.001; 95% CI: [0.048, 0.054],$p < .001$), negative movie of Study 2 (estimate[ED-EE]= 0.020 ∓0.001; 95% CI: [0.018, 0.021],$p < .001$) and neutral movie of Study 1 (estimate[ED-EE]= -0.002 ∓0.001; 95% CI: [-0.005, 0.001], $p < .001$) see Fig. 1.

As a next step, we aimed to capture a group signature that reflects the number of collective shifts of subjective emotional intensity (EE/ED) that subjects experience throughout the course of movie viewing. To do so, we used a sliding window of 40s with 1s time steps to count the number of emotional shifts across all individuals. This analysis resulted in two group time courses (EE and ED), here called group EE and ED dynamics index (Fig.3). These indices were then convolved with the hemodynamic response function (HRF). To assess the functional architecture underlying these emotional response patterns, we employed a dynamic functional connectivity (dynFC) approach. This involved using a tapered sliding window of 40s with a time step of 1 TR, computing Pearson's correlation between BOLD time courses of each pair of 214 ROIs (200 from Schaefer et al. (2018), 8 subcortical regions from Harvard-Oxford structural subcortical atlas (Kennedy et al., 2016) and 6 from insula sub-regions (Deen et al., 2011).

Generalizable Multivariate Patterns of Emotional Engagement and Disengagement

For each of the three movie clips individually, we then used a leave-one-subject-out (LOO) cross-validation approach to predict a group response of EE and ED based on each subject's dynFC patterns using nonlinear SVR models. To assess prediction accuracy, we computed the average of Fisher's z–transformed Pearson's correlations between the predicted and observed EE dynamics throughout all cross-validation runs. Features were selected based on which dynFC patterns significantly correlated with EE or ED group responses. Significance was then assessed with a one-sample t-test, testing if the observed correlation coefficients were significantly different from zero, with $p < 0.01$.

For all three movie clips (negative and neutral in Study 1 and negative in Study 2), SVR models predicted emotional group responses at levels above chance (EE: negative movie of Study 1: $r = 0.823, p < 0.001; MSE = 0.454, R^2 = 0.546$; negative movie of Study 2: $r = 0.722, p < 0.001; MSE = 0.552; R^2 = 0.448$; neutral movie of Study 1: $r = 0.618, p < 0.005; MSE = 0.663, R^2 = 0.337$; ED: 21 Grams: $r = 0.689, p < 0.001; MSE = 2.673; R^2 = 0.331$; negative movie of Study 2: $r = 0.593, p < 0.001; MSE = 8.444; R^2 = 0.302$; neutral movie of Study 1: $r = 0.516, p < 0.005; MSE = 0.778, R^2 = 0.222$).

The primary goal of this study was to uncover dynFC patterns capable of predicting a dynamic group index of EE and ED during viewing of movies that induce high levels of emotional intensity. To ensure the robustness of our findings, we investigated whether the neural features predicting emotional shifts were generalizable and not specific to the idiosyncrasies of a particular movie clip. If the predictions prove successful across negative contexts while failing in predictions between negative and neutral stimuli, it would indicate a potential specificity to contexts with high emotional intensity (Fig. 2).

First, we tested predictions across negative clips. The model trained on dynFC of subjects watching the negative clip of Study 2 successfully predicted the EE group dynamics index in the negative clip of Study 1 ($r = 0.572; p < 0.005, MSE = 50.84, R^2 = -1.30$), as did predictions in the opposite direction (negative clip of Study 1 to negative clip of Study 2: $r = 0.299; p = 0.005, MSE = 296.03, R^2 = 0.061$). The model trained on dynFC of subjects watching the neutral clip of Study 1 successfully predicted the EE group dynamics index in the negative clip of Study 1 ($r = 0.334; p = 0.005, MSE = 30.8, R^2 = -0.389$). , as did predictions in the opposite direction (negative clip of Study 1 to neutral clip of Study 1: $r = 0.18; p = 0.024, MSE = 14.553, R^2 = -45.167$). The model trained with the negative clip of Study 2 did not predict the neutral clip ($r = -0.144; p = 0.999, MSE = 99.432, R^2 = -314.827$), similarly in the opposite direction (neutral clip of Study 1 to negative movie of Study 2): $r = -0.028; p = 0.791, MSE = 401.26, R^2 = -0.272$. Together these findings imply that EE demonstrates a tendency to generalize across contexts of varying emotional intensity.

The model trained on dynFC patterns of subjects watching the negative clip of Study 2 successfully predicted the group dynamics index for ED in the negative clip of Study 1 ($r = 0.233, p = 0.005; MSE = 4.497; R^2 = -0.357$), as did predictions in the opposite direction (negative clip of Study 1 to negative clip of Study 2: $r = 0.167, p = 0.005; MSE = 13.673; R^2 = -0.128$). However, predictions between negative movie clips (Study 1 and 2) with the neutral movie clip of Study 1 failed (from the negative clip of Study 1 to the neutral clip of Study 1: $r = -0.025, p = 0.59; MSE = 1.482; R^2 = -0.273$; from the negative clip of Study 2 to the neutral clip of Study 1: $r = 0.014, p = 0.60; MSE = 5.891; R^2 = -4.184$; neutral movie clip of Study 1 to negative clip of Study 1:$r = -0.109, p = 0.96; MSE = 1.344; R^2 = -0.324$), neutral movie clip of Study 1 to negative clip of Study 2: $r = -0.009, p = 0.42; MSE = 15.243; R^2 = -0.257$).

Together these findings demonstrate successful generalization across different narratives and participants for clips inducing high levels of emotional intensity, but not for neutral contexts.

Next, we sought to characterize ROI-pairs that significantly predicted the EE and ED group dynamics index with regard to their assignment to canonical brain networks. To do so, we divided the number of significant connections by the total number of possible connections within each network. This was done for each movie clip and emotional shift type (EE vs. ED) separately; Fig. 4A.

For the negative clip of Study 1, the number of connections *positively* correlated with the EE group dynamics index mainly belonged to Visual-Visual (52%) and the DAN-Visual (10%) network pairs. The number of connections *negatively* correlated with the EE group dynamics index mainly belonged to the Salience Network (SAL)-Visual (21%) and the (DMN)-Visual pairs (18%). For the negative clip of Study 2, the number of connections *positively* correlated with the EE group dynamics index belonged to Visual-Visual (29%), DAN-DAN (22%), and Visual-DAN (19%) pairs. The number of connections *negatively* correlated with the EE group dynamics index mainly belonged to Visual-SAL (14%) and Somatomotor Network (SMN)-Visual (13%) pairs. For the neutral movie clip (Son's room), the number of connections *positively* correlated with the EE group dynamics index belonged to Visual-Visual (23%) and DAN-Visual (5%). The number of connections *negatively* correlated with the EE group dynamics index mainly belonged to Visual-Visual (17%) and Subcortical-Subcortical pairs (10%).

For *ED*, we found a broader distribution of connections across network pairs. For the negative clip of Study 1, the majority of *positive* connections *positively* correlated with ED, belonged to Visual-Visual (26%) and SMN-SMN (8%) regions, whereas the majority of connections *negatively* correlated with ED, belonged to SAL-Visual (8%) and Visual-CEN regions (5%). For the negative clip of Study 2, *positively* correlated connections with ED mainly belonged to SAL-SAL (17%) and SMN-SAL regions (15%), and *negatively* correlated connections with ED were in DMN-Visual (8%) and Visual-Visual regions (5%). In neutral movie clip *positively* correlated connections with ED mainly belonged to Visual-Visual (23%) and Visual-DAN (5%).

Next, we investigated which network patterns generalize across movie clips (1) within negative contexts and (2) those across negative *and* neutral contexts (Fig. 4). Exclusively within negative contexts, the number of connections that positively correlated with the EE group dynamics index were primarily concentrated in Visual-DMN connections (8%), and the number of connections that negatively correlated with the EE group dynamics index were primarily concentrated in Visual-SAL connections (8%). Across all narratives (negative and neutral), the number of connections that positively correlated with the EE group dynamics index were primarily concentrated in Visual-Visual (54%) and Visual-DAN (20%) network pairs, and the number of connections that negatively correlated with the EE group dynamics index were primarily concentrated in Visual-DMN (13%) and Vis-CEN (10%) network pairs. For ED, there were no significant effects when considering negative and neutral contexts together. In contrast, exclusively for negative movie clips, the number of connections positively correlated with ED belonged to SAL-SAL (13%) and SMN-SAL (12%) pairs, and the number of connections negatively correlated with ED belonged to SAL-SAL (13%) and SMN-SAL (12%) pairs.

Generalizable Univariate Patterns of Emotional Engagement and Disengagement

We further sought to identify brain activation patterns time-locked to moments underlying latent group features of EE and ED using Principal Component Analysis (PCA) on subjective annotations time courses. The primary objective of the PCA was to reduce the dimensionality of our continuous time courses of subjective annotations while retaining information that explains most of the variability in the complex movie experience data. This allowed us to distill the most significant patterns that drive variations in emotional responses. For the PCA, time points of subjective annotations were set as features and subject ID as observations. The first and second components explained the majority of the variance in the annotations (negative movie of Study 1: first= 29.54%, second= 23.27%; Sophie: first= 34.17%, second= 15.66%; neutral movie of Study 1: first= 27%, second= 21.5%; Fig. A4). We then identified time points of EE and ED from the first and second principal component time courses by using the same algorithm as described in section to extract rises and falls within a fluctuating signal time course.

The negative movie of Study 1 contained 11 EE time points, and 14 ED time points, with EE lasting 36 seconds and ED time points lasting 58 seconds. The negative movie of Study 2 contained 20 EE time points and 22 ED time points, with EE time points lasting 87 seconds and ED time points lasting 105 seconds. Finally, the neutral movie of Study 1 contained 12 EE phases and 10 ED time points, with EE time points lasting 56 seconds and ED time points lasting 34 seconds. We investigated brain activation patterns linked to group EE and ED during the viewing of neutral and negative movie clips. Specifically, we aimed to investigate whether these activation patterns were consistent across different negative movie clips or if they were more broadly applicable to movie clips disregarding their specific emotional intensity.

First, we used a voxel-wise brain activation group analysis with the contrast $engagement > disengagement$. For the negative movie clip in Study 1 (21 Grams), this analysis identified seven clusters that included the right temporal occipital fusiform cortex (toFC), left and right precentral gyrus (PrecG), the frontal eye fields (FEF) and the left dorsomedial prefrontal cortex (dmPFC); see supplement A1. Applying the standardized Yeo network template with 7 canonical networks, these clusters spatially correlated mostly with the Visual network (r = 0.62) and the DAN (r = 0.16). For the negative movie clip in Study 2 (Sophie's Choice), the analysis identified nine clusters of activation that survived multiple comparison correction, which included voxels in the right precuneus cortex (PcC), the right and left inferior lateral occipital cortex (ilOC), the superior lateral occipital cortex (slOC) and the bilateral to FC (see supplementary material A3 for the complete list of clusters). These regions spatially correlate mainly with the Visual network (r = 0.18), and DAN (r= 0.18). Finally, for the *neutral* movie clip in Study 1 (Son's Room), the analysis identified fourteen clusters, including the right and left slOC, right pregenual anterior cingulate cortex (pgACC), right dmPFC, and PrecG/FEF among others (supplement A5), which primarily correlated with the Visual network (r= 0.41) and the DAN (r= 0.17).

For the contrast *disengagement* > *engagement*, in the negative movie clip in Study 1 (21 Grams), this analysis identified six clusters, mainly located in the right and left middle temporal gyrus (mTG), and the superior temporal gyrus (sTG) and sulcus (sTS); see supplement A2, which primarily correlated with the DMN (r = 0.18) and SMN (r=0.04). For the negative movie clip in Study 2 (Sophie's Choice), five clusters were identified, with activations mainly located in the right LinG, the left and right anterior superior temporal gyrus (asTG), the mTG, and the preCG/FEF (supplement A4), which correlated with the Visual (r = 0.22) and SMN (r = 0.16). Finally, for the *neutral* movie clip in Study 1 (Son's Room) three clusters were identified, i.e. in the left Helsch's gyrus, the right superior temporal gyrus, and the left precuneus, with a spatial correlation to SMN (r=0.4) and DMN (r=0.04).

To assess the consistency of activation patterns across movie clips, we performed a conjunction analysis. This method, grounded in the composite null hypothesis, involves identifying significant activation in two conditions. It does so, by comparing the minimum statistic of voxel-wise statistical values for each condition to a threshold (Z = 2.3). Regions where the minimum statistic surpasses this threshold are deemed part of the conjunction (Nichols et al., 2005; Price & Friston, 1997). For the *engagement* > *disengagement* contrast, common activity patterns were located in the bilateral PcC, the bilateral fusiform gyrus, the bilateral slOC, and ilOC, mainly overlapping with the Visual network (r=0.25) and DAN (r=0.17). For the *disengagement* > *engagement* contrast, common activity patterns were located within the left anterior superior temporal gyrus (sTG) and right middle temporal gyrus (mTG), mainly overlapping with the DMN (r=0.09) and SMN (r=0.07).

Material and Methods

Data Sources

We analyzed both fMRI and behavioral data from two distinct independent studies that employed similar paradigms and data acquisition methods. It is important to note that the research questions addressed in these previous studies were entirely unrelated to the focus of our current investigation. For the sake of clarity, we will herein refer to these studies as Study 1 or data set 1 (Borchardt et al., 2018) and Study 2 or data set 2 (Raz et al., 2016), respectively.

Participants

Study 1 comprised twenty-two healthy female volunteers aged 20-49 years (mean age 28.1 ∓ 6.5), participants underwent screening for the absence of neurological or psychiatric disorders using the short version of the Structured Clinical Interview for DSM-IV (SCID; Wittchen et al. (1997). The study protocols were in accordance with the latest version of the Declaration of Helsinki and approved by the institutional review board of the Charité, Germany. Study 2 comprised data from forty-five participants (25 females, 19 males) aged 21-37 years (mean age 26.73 ∓ 4.69). None of the participants had a known history of neurological or psychiatric disorders. All participants provided written informed consent, and the study received approval from the ethics committees of the Tel Aviv Sourasky Medical Center.

Naturalistic viewing paradigm

In Study 1, participants watched an excerpt from the movie "21 Grams" (Iñárritu, 2003) which presents a mother learning about the death of her two daughters in a car accident (total duration: 4.45 minutes). As a neutral condition, an excerpt from the movie "Son's Room" (Moretti, 2001) was shown where scenes of a family are presented in daily life (e.g., having a casual conversation at the dinner table, reading the paper; total duration: 4.54 minutes). This movie was selected as a comparison condition to include similar lower-level features such as the appearance of human faces and domestic scenes (4.54 minutes). Movie clips were shown in the dubbed German version. In Study 1, subjects rated the negative clip significantly of higher negative valence and arousal as compared to the neutral clip (see Borchardt et al., 2018). The two film clips have been used in previous studies for negative and neutral emotion induction, respectively (2018; Gaviria et al., 2021; Hanich et al., 2014).

In Study 2, participants viewed an excerpt from the movie *Sophie's Choice* (Pakula, 1983), depicting a mother facing the harrowing decision of choosing which of her two children to save from certain death. (total duration: 10.00 minutes). This film clip has been used in previous studies to induce sadness (Innes-Ker, 2015; Raz et al., 2016).

Subjective continuous emotional intensity annotations

Participants in Study 1 underwent a two-stage movie-watching process within an fMRI environment. Initially, they viewed the neutral and the negative movie clips in a counterbalanced order during fMRI scanning. Subsequently, approximately 15 minutes post-scanning, subjects rewatched both movie clips outside the scanner environment (experimental room) while concurrently providing continuous emotional intensity ratings for their emotional experiences during the initial fMRI viewing. The continuous emotional intensity annotations were collected using a trackball-operated mouse interface. Adjacent to the video playback, a visual analog scale (VAS) with a range from 0 ("not at all") to 250 ("very much") was displayed. Participants manipulated the trackball to adjust VAS values according to their emotional experience. The instruction provided was as follows: "Following, are 2 short ratings of the movie clips that you previously watched. You are going to see both movie clips again on the PC screen and are subsequently asked to rate how emotional you felt while watching" (German original in supplements). Emotionality annotations were sampled at a frequency rate of 30Hz and subsequently downsampled to match the fMRI sampling rate of 0.5Hz for data compatibility.

In Study 2, participants underwent a similar experimental procedure as in Study 1. Initially, participants viewed the movie clip while undergoing fMRI scanning. Approximately 15 minutes following the scanning session, participants were instructed to watch the same movie clip outside the scanner environment (experimental room). During this period, they provided continuous emotional intensity ratings, following the guidelines as in Study 1. To gather these subjective annotations, participants employed a 7-point Likert scale, with values ranging from 0 (representing "neutral") to 7 (indicating "very intense"). This Likert scale was finely divided, comprising three sublevels within each main level. Consequently, participants had to register their responses three times to progress to the subsequent main level of emotional intensity (for details, see Raz et al. 2016). As in Study 1, we sampled emotional intensity ratings at a frequency rate of 10Hz. Subsequently, to ensure alignment with the fMRI data, we downsampled the annotations to match the fMRI sampling rate of 0.33Hz.

Calculation of Engagement and Disengagement

Engagement and disengagement moments in time were extracted by using an algorithm previously employed to separate four phases of a temporal signal (trough, rise, peak, fall) Dessu et al. (2020); Kato et al. (2015); Shine et al. (2019). Accordingly, EE and ED periods were defined as rises and falls within the temporal fluctuations of subjective emotional intensity. To count as an EE or ED period, an emotional intensity score had to be within a certain range (the 33rd and 67th percentile) and (2) exhibit a positive and a negative change between 2 subsequent time points for EE and ED, respectively.

Group response of emotional engagement and disengagement. Our objective was to examine the functional architecture associated with the frequency of simultaneous reports of EE or ED across individuals at a given moment in time. In simpler terms, we aimed to create a group time course where each time point represented the number of moments when individuals reported EE or ED. To achieve this, we initially utilized the algorithm mentioned to process individual continuous annotations, resulting in two binary time courses for each individual. One of these time courses indicated the presence of EE, while the other indicated the presence of ED at every moment in time.

Using a sliding window approach (window size of 40s; time step of 1 TR) we counted the number of EE moments present across all individuals for a sliding window in time. The same procedure was repeated for ED, resulting in one group signature time course for EE and one for ED. The group EE and ED time course was then convolved with the HRF. These convolved time courses were then employed in conjunction with actual fMRI data to train and test SVR models. This approach of calculating fluctuations of an emotional group response enables us to extract information on both the similarity between individuals' subjective experiencing *and* directionality (higher and lower frequency of EE/ED reports).

Image acquisition

In Study 1, functional MRI images were acquired on a Siemens Trio 3-T scanner (Siemens, Erlangen, Germany) with a twelve-channel radiofrequency head coil, using a T2*-weighted Echo Planar Imaging (EPI) sequence (repetition time (TR)/error time(TE) = 2,000/30 ms, flip angle = 70°, 64 × 64 matrix, field of view (FOV) = 192 × 192 mm^2, in-plane resolution = 3 mm^2, slice thickness = 3mm, 37 axial slices). The natural-viewing sessions consisted of 147 volumes. T1-weighted anatomical reference images were acquired using 3D-MPRAGE sequence (176 sagittal slices covering the whole brain, 1 mm^3 isotropic resolution, TR/TE

= 1900/2.52 ms, 9° flip angle, 256 × 256 matrix).

In Study 2, functional MRI images were obtained by a GE 3-T Signa Excite echo speed scanner with an eight-channel head coil located at the Wohl Institute for Advanced Imaging at the Tel Aviv Sourasky Medical Center. Functional whole-brain scans were performed in interleaved order with a T2*-weighted gradient EPI pulse sequence (TR/TE = 3,000/35 ms, flip angle = 90°, pixel size = 1.56 mm, FOV = 200 × 200 mm, slice thickness = 3 mm, 39 slices per volume). The structural scans included a T1-weighted 3-D axial spoiled gradient echo (SPGR) pulse sequence (TR/TE = 7.92/2.98 ms, 150 slices, slice thickness = 1 mm, flip angle = 15°, pixel size = 1 mm, FOV = 256 × 256 mm). Active noise-cancelling headphones (Optoacoustic) were used. (Taken from Raz et al., 2016)

Image preprocessing

Both data sets were preprocessed using fMRIprep 1.3.2 (Esteban et al., 2019), which is based on Nipype 1.1.9 (K. Gorgolewski et al., 2011; K. J. Gorgolewski et al., 2019). The pipeline includes slice time and motion correction, susceptibility distortion correction, realignment, smoothing, and registration to common space. ICA-AROMA was performed to identify and remove motion-related components (Pruim et al., 2015). Physiological nuisance was corrected by extracting the mean time course of cerebrospinal fluid (CSF) and white matter (WM) calculated from the preprocessed images. The first two volumes of fMRI sequence of movie clips in sample 1 were discarded to avoid T1 saturation effect. The last four volumes of fMRI during the negative movie clip (samples one and two) were removed, given that the clip length was shorter than the entire scan session. One subject from sample one was discarded due to excessive head movement, identified with mean frame-wise displacement (threshold = 0.20) resulting in 21 participants. Applying the same cut-off to Study 2, three subjects were discarded resulting in forty-four participants in the final sample.

Image analysis

Dynamic predictive modeling of emotional cinematic experience. Our main research aim was to identify dynamic functional connectivity patterns predictive of a group response of EE in and ED from emotionally intense negative content that generalizes across different narratives. To extract dynamic functional connectivity patterns, for every participant, we extracted BOLD time courses using a 200 region parcellation by Schaefer et al. (2018), the Harvard-Oxford structural subcortical atlas (8 regions) Kennedy et al. (2016) and insula sub-regions (6 regions) Deen et al. (2011) resulting in a total of 214 brain regions). Next, we calculated dynFC of BOLD time series, computed as the Pearson correlation between pairs of regions (214 x 214 ROIs), using a tapered sliding window with a length of 40 seconds and a tapering factor of 1 TR.

In the next step, we aimed to investigate if the number of inter-regional connections can predict a dynamic group response of EE and ED, respectively. First, we selected neural features based on the correlation between ROI-pairs connections and the group response of either EE or ED. The significance of this correlation was determined through a one-sample t-test ($p<0.01$). We then used SVR with a radial basis function (RBF) kernel to predict the group response of either EE or ED based on these multivariate features in each subject's functional architecture. Next, we did a leave-one-out (LOO) cross-validation with a maximum iteration set to 1,000 to fit a model on the train data and predict on test data (sklearn.svm.SVR in Python). For every LOO run, the subject's test data was excluded for the calculation of the group EE and ED response time courses (see methods). We then evaluated the predictive performance of the cross-validated models by using Pearson correlation between the predicted and the empirical scores for each participant. To determine the mean prediction accuracy, we utilized Mean Squared Error (MSE) and the coefficient of determination (r-squared). This allowed us to estimate three metrics for the sake of comparison: MSE, r-squared, and r. Treating each subject prediction as an independent sample within the model, we computed these three metrics individually for each subject. To represent the group collectively, we calculated the mean value for each metric.

Between movie prediction. To assess the generalizability of neural patterns related to EE and ED in emotionally intense narratives, independently of specific movie characteristics, we examined whether the neural features used to predict group EE responses in one negative movie clip could predict group EE responses in a different negative movie clip from an independent study. To further test generalizability in various valenced contexts, successful predictions would need to extend across both negative and neutral narratives *and* participants. Specifically, this would involve predictions between the neutral narrative and the emotionally intense narratives (Fig. 2A).

We selected the Pearson correlation as a metric for evaluating our prediction performance, aligning with the approach employed by Song et al. (2021). Our interest lies in ensuring that the model captures the temporal dynamics of group EE and ED. To assess the significance of the empirical mean correlation values, we computed the percentage of simulated correlation values resulting from the SVR phase-randomized EE and ED. The threshold was set to ensure that this percentage did not surpass 95% ($p < 0.05$); Fig. 2B. This iterative procedure was repeated 200 times. Throughout this section's analyses, we employed a modified version of the dynamic predicting modeling code initially developed by Song et al. (2021).

Engagement and Disengagement networks. We further investigated which canonical networks were primarily involved in predicting emotional responses. To this aim, we grouped ROI-pairs that significantly contributed to the model into seven canonical functional networks based on a parcellation by Yeo et al. (2011). We then calculated the proportion of all participants' connections within a particular network, specifically those connections responsible for predicting emotional responses. First, we divided the number of significant connections in one specific network by the total number of connections within that network. To evaluate the relevance of one network in predicting emotional responses

(EE and ED frequency), we generated null matrices through the phase-randomization of empirical emotional response time courses. This process involves transforming the original data into the frequency domain, randomizing the phases, and subsequently converting the data back into the time domain, thus generating surrogate data with equivalent second-order properties as the original time series (Gias, 2023). These randomized data sets were used as input for the SVR model to generate simulated predictions, thus forming the null distribution. To evaluate the significance of empirical mean r values, we calculated the percentage of network pairs from the randomized data that surpassed the observed proportion of network pairs in the empirical data. This comparison ensured that the observed proportion did not exceed 99%, signifying statistical significance ($p < 0.01$); Fig. 4A.

To assess effects that were not reliant on the particular movie context, we superimposed the significant network pairs from all the movie clips. This was done to pinpoint consistent patterns across emotionally intense movie clips and neutral/low-intensity movie clip (Fig. 4B). Our second objective entailed identifying the substantial pairs of regions within the model (those predictive of EE and ED across movie clips) according to the following criteria: 1) The connections that manifested in over 50% of the subjects, 2) The ROI-pairs connections that were significant for at least 2 movie clips. For visualization, we selected the two nodes with the greatest number of ROI-pairs connections (Fig. 4C).

Furthermore, we sought to enhance the insights from the activation analysis by exploring the connectivity patterns of regions identified through that process. Employing the same criteria delineated above, we pinpointed regions that concurred with the outcomes of the previous analysis (Fig. A3).

Time-locked brain signal intensity patterns. Our second research aim was to identify brain activation patterns time-locked to moments when the group mutually experienced moments of EE and ED, respectively. To assess the underlying brain activation patterns we performed a voxel-wise activation analysis over the two independent data sets. Preprocessed functional brain images were analyzed using a two-level GLM approach using FEAT version 6.0, a part of FMRIB Software Library version (FSL version 6.0.3; www.fmrib.ox.ac.uk/fsl; Jenkinson et al. (2012). For the first level analysis, we employed the first component obtained through PCA across subjective emotional intensity annotations, as the main regressor for both EE and ED (see methods). This was used to create two contrasts: (1) EE > ED and (2) ED > EE (Fig. 5B). These contrasts were modeled as a single-event stimulus, with one entry per timepoint, and were convolved with the HRF (gamma variate). We also include the second component as a covariate, since they contained a considerable proportion of variance in the group response (negative movie of Study 1: 23%; negative movie of Study 2 15%; Son's room: 22%). For the group-level analysis, one sample t-test was used. Gaussian Random Field Theory is used for cluster-based thresholding to control the family-wise error rate at both the subject and group levels of analysis (Z > 3.1 and $\alpha = 0.05$) Woolrich et al. (2004).

GLM Conjunction analysis. Subsequently, we sought to identify shared brain activation patterns among emotionally intense narratives and how they might differ from the neutral narrative. To accomplish this, we conducted a formal conjunction analysis, by identifying voxels with significant conjoint effects across different data sets (see Nichols et al., 2005; Price and Friston, 1997). As an example, contrasts were calculated as Study 1/negative movie ($Engagement > Disengagement$)$\cap$ Study 2/negative movie ($Engagement > Disengagement$). This produced a conjunction of statistical maps thresholded at Z = 2.3 and $\alpha = 0.001$. To identify the networks represented by the resulting areas, spatial correlation between the functional canonical networks (Yeo et al., 2011) and the conjunction image was performed.

Discussion

In this study, we aimed to identify neural signatures of EE and ED during movie viewing. We analyzed data from two independent studies, combining fMRI with subjective annotations. Our findings suggest that EE and ED during movie viewing are associated with distinct brain activation and connectivity patterns. In negative movie clips, more simultaneous ED reports were linked to increased between-network connections, while more simultaneous EE reports were linked to reduced between-network connections. This opposing pattern may suggest that ED involves regulatory cognitive processes needing extensive network communication (Cohen & D'Esposito, 2016; Morawetz et al., 2020), while EE may relate to reduced cognitive control and enhanced immersion in emotionally salient movie material. A model trained to predict ED based on neural features in one negative movie clip successfully predicted ED in another negative movie clip, even when the movie clips were from independent samples with different narratives. However, this predictive ability did not extend to neutral contexts, implying some specificity to negative content. EE activated regions in the DAN and visual areas, possibly reflecting visual attention to emotionally salient stimuli. In contrast, ED drew on ventral DMN regions, possibly supporting the evaluation of emotional material, needed for emotion regulation. In summary, our results indicate that emotional movie viewing elicits consistent brain states that can be traced with subjective assessments of emotional experiences.

Our main objective was to assess whether (1) a model trained on dynFC to predict a group EE and ED dynamics index in one movie clip was predictive of a group EE and ED dynamics index in another movie clip and if so, (2) if the predictability is specific to negative and fails for neutral content. Given that Study 1 included both a negative and a neutral clip from the same individuals, and Study 2 featured a negative movie clip from an entirely independent sample with a different narrative, we hypothesized that meeting condition (2) would be adequate to infer some degree of specificity for emotional, as opposed to neutral, movie clip content. Our results indicate that both conditions were met for ED, providing support for emotional specificity in this aspect. However, these conditions failed to hold for EE, suggesting a divergence in the mechanisms underlying EE and ED across different movie contexts (Fig. 5B).

Disengagement. In general, group ED dynamics were predominantly predicted by widespread increases of between-network connections. The most substantial effects were observed with a greater number of connections within the SAL and between SAL and the SMN. Previous research has linked the strength of SAL-SMN coupling to somatic arousal related to anxiety (Wu et al., 2019) and the attention directed toward interoceptive markers of arousal, such as heart rate (Critchley et al., 2004). In our study, the recruitment of connections between SAL and SMN during negative emotional movies could indicate an intensified focus on individuals' bodily sensations induced by intense emotional experiences. This heightened interoception may be a relevant factor influencing ED. Specifically, as individuals direct their attention away from emotional stimuli. In this state they may become more internally focused paying attention to their bodily sensations as they process the emotional experience. Notably, a key hub that exhibited the highest number of connections in predicting group ED dynamics was the ventromedial prefrontal cortex (vmPFC). This region has been implicated in both the generation and regulation of negative emotions, with converging evidence suggesting it may function as a relay for generalizable representations of negative emotions (Kragel et al., 2018). Since the highly connected nodes were exclusive to negative movie clips, one could speculate that the involvement of the vmPFC may support the regulation of negative emotions induced by the negative movie clips.

Engagement. While cross-movie predictions for ED exhibited some specificity to negative movie content, interpretations regarding emotional specificity for EE remained inconclusive. Successful predictions were not limited to negative content but extended to both negative and neutral movie clips. Notably, this pattern emerged when presented to the same individual but did not hold across independent individuals.

A greater number of connections within the visual network, as well as between the visual network and the DAN were predictive of group EE. Prior discussions have emphasized the significance of disentangling the involvement of the DMN from the visual network regarding its role for attention processes. The DMN plays a crucial role in facilitating DAN-Visual connectivity, a process vital for directing attention toward external salient stimuli (Anticevic et al., 2012).

In our study, we observed a subset of visual to DAN connections that predicted opposing patterns in group EE. This suggests that these networks are implicated not only in promoting EE but also in its reduction. Prior research has also demonstrated that the coupling between the visual cortex and various networks varies depending on the specific task requirements (Chadick & Gazzaley, 2011). In certain cognitive processes, there is a positive coupling between segments of the visual cortex and components of the DMN (2011; Daselaar et al., 2004). Conversely, in scenarios where the DMN is activated by other cognitive processes, there is concurrent suppression observed in the visual cortex (Shulman et al., 2007; Smallwood et al., 2012). Previous findings have indicated that differential connectivity patterns between the DMN and the visual network predict emotional states such as sadness or happiness during movie viewing (Xu et al., 2023). This emphasizes the involvement of these networks in emotional experiencing within naturalistic scenarios. Nevertheless, further research is needed to investigate the specific brain regions implicated and the directionality of connectivity strength.

Next, our our objective was to identify brain activation patterns associated with temporal markers reflecting latent group features of EE and ED. None of the brain activation patterns were specific to the negative movie clips but instead extended to the neutral one. Here we report results that were consistent across all three movie clips. Our results reveal that EE was associated with heightened activation in the dorsal precuneus extending into the posterior cingulate cortex, which is a part of the DAN(Yeo et al., 2011). The precuneus, often assigned to the DMN, is often reported to be activated during movie viewing. For instance, disrupting or scrambling the narrative in movies, and thus impeding EE, leads to reduced precuneus connectivity as compared to when the narrative remains intact (Deng et al., 2019).

Prior research reported increased activations in this region when attention shifts, and these activations independently account for changes in reward magnitude in a visual search task (Tosoni et al., 2013). In our study, enhanced activation during EE could reflect a shift in attention towards emotionally salient stimuli and/or an expected shift in reward magnitude. Both factors are essential for following the movie narrative. For example, a scene where the protagonist cannot find her children at home and suddenly receives a phone call, would let the viewer shift the attention towards the phone call. The unexpected phone call introduces uncertainty, evoking diverse emotional responses like relief, anxiety, or surprise, thereby influencing the perceived reward magnitude and contributing to the variability in expected reward levels for the viewer. The study by Tosoni et al. also found that the visual cortex is sensitive to reward expectancy, particularly related to specific locations in the visual field. This could potentially explain why EE involves heightened activations in visual regions such as the bilateral superior and inferior occipital cortex (slOC and ilOC). Stimuli at specific locations might induce higher reward expectancy in the movie viewer. Furthermore, the affect-biased attention model by Mohanty et al. (2008) posits that spatial and emotional information is integrated at early stages of sensory processing in the visual cortex, specifically within the fusiform gyrus, to facilitate top-down modulation of visual cortical regions (Mohanty & Sussman, 2013). Additionally, the fusiform gyrus was found to cooperate with visual areas such as the slOC and ilOC to direct attention towards emotionally relevant information in space (Pessoa et al., 2002; Pourtois et al., 2005). In contrast to EE, which activated brain regions supporting visual attention, ED was associated with higher activations within DMN regions, such as the bilateral middle temporal gyrus and superior temporal lobes. As mentioned earlier, we hzpothesized that ED might be associated with a redirection of attention from external stimuli towards an internal state of emotion evaluation, potentially involving processes related to emotion regulation. Previous research showed that the induction of sadness resulted in more analytical emotion regulation strategies compared to when other negative emotions like anger are experienced (Bodenhausen et al., 1994). The superior temporal gyrus (STG) plays a pivotal role as a socio-emotional contextualization node, particularly when viewers engage with movies requiring the interpretation of social interactions between characters. To effectively comprehend these perceived social interactions, individuals needed to tap into their pre-existing social conceptual knowledge (Bukowski & Lamm, 2020; Ross & Olson, 2010; Zahn et al., 2007; Zahn et al., 2009). These processes involve higher-level processes involving recognition, understanding, and reasoning about oneself and others, with implications for predicting behavior (Bukowski & Lamm, 2020), particularly in naturalistic contexts when compared to various lower and higher-level features (Masson & Isik, 2021).

Limitations

The use of multiple independent data sets for a common research objective bears limitations. The data sets differed in cultural backgrounds and functional image acquisition methodologies and subjective annotation schemes varied. Specifically, one group utilized continuous pointer movements on a bar, while the other used double button presses to indicate a subjective change of emotional intensity. Nevertheless, we found a considerable consistency of results across data sets. Additionally, the study's scope was confined to movie clips with a sad affective tone, which may raise concerns about generalizability to other emotions. However, the inclusion of a neutral movie clip in the analysis enabled the assessment of neural patterns underlying emotional content processing.

Conclusion

We used retroactive emotional intensity annotations and fMRI during movie viewing to track neural responses underlying EE and ED. Using this approach, we showed across independent fMRI movie clip-watching data sets that distinctive neural response patterns characterize EE and ED. Taken together, these results suggest that EE and ED may be supported by dynamic reconfiguration of neural activation patterns.

References

Anticevic, A., Cole, M. W., Murray, J. D., Corlett, P. R., Wang, X.-J., & Krystal, J. H. (2012). The role of default network deactivation in cognition and disease. *Trends in cognitive sciences*, *16*(12), 584–592.

Bodenhausen, G. V., Sheppard, L. A., & Kramer, G. P. (1994). Negative affect and social judgment: The differential impact of anger and sadness. *European Journal of social psychology*, *24*(1), 45–62.

Borchardt, V., Fan, Y., Dietz, M., Melendez, A. L. H., Bajbouj, M., Gärtner, M., Li, M., Walter, M., & Grimm, S. (2018). Echoes of affective stimulation in brain connectivity networks. *Cerebral Cortex (New York, N.Y.: 1991)*, *28*. https://doi.org/10.1093/cercor/bhx290

Bukowski, H., & Lamm, C. (2020). Superior temporal sulcus. *Encyclopedia of personality and individual differences*, 5316–5319.

Chadick, J. Z., & Gazzaley, A. (2011). Differential coupling of visual cortex with default or frontal-parietal network based on goals. *Nature neuroscience*, *14*(7), 830–832.

Cohen, J. R., & D'Esposito, M. (2016). The segregation and integration of distinct brain networks and their relationship to cognition. *Journal of Neuroscience*, *36*(48), 12083–12094.

Critchley, H. D., Wiens, S., Rotshtein, P., Öhman, A., & Dolan, R. J. (2004). Neural systems supporting interoceptive awareness. *Nature neuroscience*, *7*(2), 189–195.

Daselaar, S. M., Prince, S. E., & Cabeza, R. (2004). When less means more: Deactivations during encoding that predict subsequent memory. *Neuroimage*, *23*(3), 921–927.

Deen, B., Pitskel, N. B., & Pelphrey, K. A. (2011). Three systems of insular functional connectivity identified with cluster analysis. *Cerebral cortex*, *21*(7), 1498–1506.

Deng, Z., Wu, J., Gao, J., Hu, Y., Zhang, Y., Wang, Y., Dong, H., Yang, Z., & Zuo, X. (2019). Segregated precuneus network and default mode network in naturalistic imaging. *Brain Structure and Function*, *224*, 3133–3144.

Dessu, S. B., Price, R. M., Kominoski, J. S., Davis, S. E., Wymore, A. S., McDowell, W. H., & Gaiser, E. E. (2020). Percentile-range indexed mapping and evaluation (prime): A new tool for long-term data discovery and application. *Environmental Modelling & Software*, *124*, 104580.

Esteban, O., Markiewicz, C. J., Blair, R. W., Moodie, C. A., Isik, A. I., Erramuzpe, A., Kent, J. D., Goncalves, M., DuPre, E., Snyder, M., Oya, H., Ghosh, S. S., Wright, J., Durnez, J., Poldrack, R. A., & Gorgolewski, K. J. (2019). fMRIPrep: A robust preprocessing pipeline for functional MRI. *Nature Methods*, *16*(1), 111–116. https://doi.org/10.1038/s41592-018-0235-4

Gaviria, J., Rey, G., Bolton, T., Delgado, J., Van De Ville, D., & Vuilleumier, P. (2021). Brain functional connectivity dynamics at rest in the aftermath of affective and cognitive challenges. *Human brain mapping*, *42*(4), 1054–1069.

Gias, C. (2023). CVX: Phase randomization: Simultaneous phase randomization of a set of time series, version 1.0.0.0.

Gorgolewski, K., Burns, C. D., Madison, C., Clark, D., Halchenko, Y. O., Waskom, M. L., & Ghosh, S. S. (2011). Nipype: A flexible, lightweight and extensible neuroimaging data processing framework in python [Publisher: Frontiers]. *Frontiers in Neuroinformatics*, *5*. https://doi.org/10.3389/fninf.2011.00013

Gorgolewski, K. J., Esteban, O., Markiewicz, C. J., Ziegler, E., Ellis, D. G., Jarecka, D., Johnson, H., Notter, M. P., Burns, C., Manhães-Savio, A., Hamalainen, C., Yvernault, B., Salo, T., Goncalves, M., Jordan, K., Waskom, M., Wong, J., Modat, M., Clark, D., . . . Ghosh, S. (2019, September 7). *Nipy/nipype: 1.2.2.* Zenodo. https://doi.org/10.5281/zenodo.3402255

Gross, J. J. et al. (2014). Emotion regulation: Conceptual and empirical foundations. *Handbook of emotion regulation*, *2*, 3–20.

Hanich, J., Wagner, V., Shah, M., Jacobsen, T., & Menninghaus, W. (2014). Why we like to watch sad films. the pleasure of being moved in aesthetic experiences [Place: US

Publisher: Educational Publishing Foundation]. *Psychology of Aesthetics, Creativity, and the Arts*, *8*(2), 130–143. https://doi.org/10.1037/a0035690

Hox, J., Moerbeek, M., & Van de Schoot, R. (2017). *Multilevel analysis: Techniques and applications*. Routledge.

Hutcherson, C., Goldin, P. R., Ochsner, K. N., Gabrieli, J., Barrett, L. F., & Gross, J. J. (2005). Attention and emotion: Does rating emotion alter neural responses to amusing and sad films? *Neuroimage*, *27*(3), 656–668.

Iñárritu, A. G. (2003). *21 grams* [Translated title: 21 Grams , event-location:].

Innes-Ker, Å. (2015). Film and music in laboratory experiments: Emotion induction. *Music and the Moving Image*, *8*(2), 58–68.

Jenkinson, M., Beckmann, C. F., Behrens, T. E., Woolrich, M. W., & Smith, S. M. (2012). Fsl. *Neuroimage*, *62*(2), 782–790.

Kato, S., Kaplan, H. S., Schrödel, T., Skora, S., Lindsay, T. H., Yemini, E., Lockery, S., & Zimmer, M. (2015). Global brain dynamics embed the motor command sequence of caenorhabditis elegans. *Cell*, *163*(3), 656–669.

Kennedy, D., Haselgrove, C., Fischl, B., Breeze, J., Frazier, J., Seidman, L., Goldstein, J., & Kosofsky, B. (2016). Harvard-oxford cortical and subcortical structural atlases. *Harvard Center for Morphometric Analysis*.

Koval, P., Brose, A., Pe, M. L., Houben, M., Erbas, Y., Champagne, D., & Kuppens, P. (2015). Emotional inertia and external events: The roles of exposure, reactivity, and recovery. *Emotion*, *15*(5), 625.

Koval, P., Butler, E. A., Hollenstein, T., Lanteigne, D., & Kuppens, P. (2015). Emotion regulation and the temporal dynamics of emotions: Effects of cognitive reappraisal and expressive suppression on emotional inertia. *Cognition and Emotion*, *29*(5), 831–851.

Kragel, P. A., Kano, M., Van Oudenhove, L., Ly, H. G., Dupont, P., Rubio, A., Delon-Martin, C., Bonaz, B. L., Manuck, S. B., Gianaros, P. J., et al. (2018).

Generalizable representations of pain, cognitive control, and negative emotion in medial frontal cortex. *Nature neuroscience*, *21*(2), 283–289.

Kuppens, P., & Verduyn, P. (2015). Looking at emotion regulation through the window of emotion dynamics. *Psychological Inquiry*, *26*(1), 72–79.

Li, T., Baveye, Y., Chamaret, C., Dellandréa, E., & Chen, L. (2015). Continuous arousal self-assessments validation using real-time physiological responses. *Proceedings of the 1st International Workshop on Affect & Sentiment in Multimedia*, 39–44.

Lieberman, M. D., Eisenberger, N. I., Crockett, M. J., Tom, S. M., Pfeifer, J. H., & Way, B. M. (2007). Putting feelings into words. *Psychological Science*, *18*(5), 421–428. https://doi.org/10.1111/j.1467-9280.2007.01916.x

Malandrakis, N., Potamianos, A., Evangelopoulos, G., & Zlatintsi, A. (2011). A supervised approach to movie emotion tracking. *2011 IEEE international conference on acoustics, speech and signal processing (ICASSP)*, 2376–2379.

Masson, H. L., & Isik, L. (2021). Functional selectivity for social interaction perception in the human superior temporal sulcus during natural viewing. *NeuroImage*, *245*, 118741.

Mohanty, A., Gitelman, D. R., Small, D. M., & Mesulam, M. M. (2008). The spatial attention network interacts with limbic and monoaminergic systems to modulate motivation-induced attention shifts. *Cerebral cortex*, *18*(11), 2604–2613.

Mohanty, A., & Sussman, T. J. (2013). Top-down modulation of attention by emotion.

Morawetz, C., Riedel, M. C., Salo, T., Berboth, S., Eickhoff, S. B., Laird, A. R., & Kohn, N. (2020). Multiple large-scale neural networks underlying emotion regulation. *Neuroscience & Biobehavioral Reviews*, *116*, 382–395.

Moretti, N. (2001, March 9). *La stanza del figlio* [Translated title: The Son's Room , event-location:].

Morgenroth, E., Vilaclara, L., Muszynski, M., Gaviria, J., Vuilleumier, P., & Van De Ville, D. (2022). Probing neurodynamics of experienced emotions-a hitchhiker's guide to film fmri.

Nastase, S. A., Goldstein, A., & Hasson, U. (2020). Keep it real: Rethinking the primacy of experimental control in cognitive neuroscience. *NeuroImage*, *222*, 117254.

Nichols, T., Brett, M., Andersson, J., Wager, T., & Poline, J.-B. (2005). Valid conjunction inference with the minimum statistic. *Neuroimage*, *25*(3), 653–660.

Pakula, A. J. (1983). *Sophie's choice*.

Pessoa, L., McKenna, M., Gutierrez, E., & Ungerleider, L. G. (2002). Neural processing of emotional faces requires attention. *Proceedings of the National Academy of Sciences*, *99*(17), 11458–11463.

Pourtois, G., Schwartz, S., Seghier, M. L., Lazeyras, F., & Vuilleumier, P. (2005). Portraits or people? distinct representations of face identity in the human visual cortex. *Journal of cognitive neuroscience*, *17*(7), 1043–1057.

Price, C. J., & Friston, K. J. (1997). Cognitive conjunction: A new approach to brain activation experiments. *Neuroimage*, *5*(4), 261–270.

Pruim, R. H. R., Mennes, M., van Rooij, D., Llera, A., Buitelaar, J. K., & Beckmann, C. F. (2015). ICA-AROMA: A robust ICA-based strategy for removing motion artifacts from fMRI data. *NeuroImage*, *112*, 267–277. https://doi.org/10.1016/j.neuroimage.2015.02.064

Raz, G., Touroutoglou, A., Wilson-Mendenhall, C., Gilam, G., Lin, T., Gonen, T., Jacob, Y., Atzil, S., Admon, R., & Bleich-Cohen, M. (2016). Functional connectivity dynamics during film viewing reveal common networks for different emotional experiences. *Cognitive, Affective, & Behavioral Neuroscience*, *16*, 709–723.

Ross, L. A., & Olson, I. R. (2010). Social cognition and the anterior temporal lobes. *Neuroimage*, *49*(4), 3452–3462.

Saarimäki, H. (2021). Naturalistic stimuli in affective neuroimaging: A review [Publisher: Frontiers]. *Frontiers in Human Neuroscience*, *0*. https://doi.org/10.3389/fnhum.2021.675068

Saarimäki, H., Glerean, E., Smirnov, D., Mynttinen, H., Jääskeläinen, I. P., Sams, M., & Nummenmaa, L. (2022). Classification of emotion categories based on functional connectivity patterns of the human brain. *NeuroImage*, *247*, 118800.

Schaefer, A., Kong, R., Gordon, E. M., Laumann, T. O., Zuo, X.-N., Holmes, A. J., Eickhoff, S. B., & Yeo, B. T. (2018). Local-global parcellation of the human cerebral cortex from intrinsic functional connectivity mri. *Cerebral cortex*, *28*(9), 3095–3114.

Scherer, K. R. (2009). The dynamic architecture of emotion: Evidence for the component process model. *Cognition and emotion*, *23*(7), 1307–1351.

Sheppes, G., & Gross, J. J. (2011). Is timing everything? temporal considerations in emotion regulation. *Personality and Social Psychology Review*, *15*(4), 319–331.

Shine, J. M., Breakspear, M., Bell, P. T., Ehgoetz Martens, K. A., Shine, R., Koyejo, O., Sporns, O., & Poldrack, R. A. (2019). Human cognition involves the dynamic integration of neural activity and neuromodulatory systems. *Nature neuroscience*, *22*(2), 289–296.

Shulman, G. L., Astafiev, S. V., McAvoy, M. P., d'Avossa, G., & Corbetta, M. (2007). Right tpj deactivation during visual search: Functional significance and support for a filter hypothesis. *Cerebral cortex*, *17*(11), 2625–2633.

Smallwood, J., Brown, K., Baird, B., & Schooler, J. W. (2012). Cooperation between the default mode network and the frontal–parietal network in the production of an internal train of thought. *Brain research*, *1428*, 60–70.

Song, H., Finn, E. S., & Rosenberg, M. D. (2021). Neural signatures of attentional engagement during narratives and its consequences for event memory. *Proceedings of the National Academy of Sciences*, *118*(33), e2021905118.

Sonkusare, S., Breakspear, M., & Guo, C. (2019). Naturalistic stimuli in neuroscience: Critically acclaimed. *Trends in cognitive sciences*, *23*(8), 699–714.

Tosoni, A., Shulman, G. L., Pope, A. L., McAvoy, M. P., & Corbetta, M. (2013). Distinct representations for shifts of spatial attention and changes of reward contingencies in the human brain. *Cortex*, *49*(6), 1733–1749.

Wittchen, H.-U., Wunderlich, U., Gruschwitz, S., & Zaudig, M. (1997). Skid i. strukturiertes klinisches interview für dsm-iv. achse i: Psychische störungen. interviewheft und beurteilungsheft. eine deutschsprachige, erweiterte bearb. d. amerikanischen originalversion des skid i.

Woolrich, M. W., Behrens, T. E., Beckmann, C. F., Jenkinson, M., & Smith, S. M. (2004). Multilevel linear modelling for fmri group analysis using bayesian inference. *Neuroimage*, *21*(4), 1732–1747.

Wu, X., Shi, L., Wei, D., & Qiu, J. (2019). Brain connection pattern under interoceptive attention state predict interoceptive intensity and subjective anxiety feeling. *Human brain mapping*, *40*(6), 1760–1773.

Xu, S., Zhang, Z., Li, L., Zhou, Y., Lin, D., Zhang, M., Zhang, L., Huang, G., Liu, X., Becker, B., et al. (2023). Functional connectivity profiles of the default mode and visual networks reflect temporal accumulative effects of sustained naturalistic emotional experience. *NeuroImage*, *269*, 119941.

Yeo, B. T., Krienen, F., Sepulcre, J., Sabuncu, M., & Lashkari, D. (2011). 551 m. hollinshead, jl roffman, jw smoller, l. zöllei, jr polimeni, 552 et al., the organization of the human cerebral cortex estimated by intrinsic 553 functional connectivity. *Journal of neurophysiology*, *106*(3), 1125–554.

Zahn, R., Moll, J., Krueger, F., Huey, E. D., Garrido, G., & Grafman, J. (2007). Social concepts are represented in the superior anterior temporal cortex. *Proceedings of the National Academy of Sciences*, *104*(15), 6430–6435.

Zahn, R., Moll, J., Paiva, M., Garrido, G., Krueger, F., Huey, E. D., & Grafman, J. (2009). The neural basis of human social values: Evidence from functional mri. *Cerebral cortex*, *19*(2), 276–283.

Zhou, F., Zhang, R., Yao, S., Dong, D., Feng, P., Kranz, G., Feng, T., & Becker, B. (2023). Capturing dynamic fear experiences in naturalistic contexts: An ecologically valid fmri signature integrating brain activation and connectivity. *bioRxiv*, 2023–08.

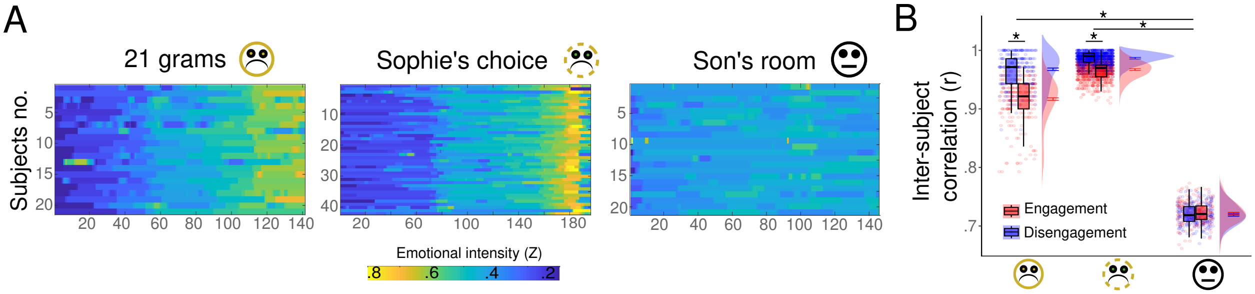

Figure 1. (A) Individual subjective emotional intensity annotations over time for each movie clip, z-scored and scaled between 0 and 1 for visualization purposes. (B) Estimated inter-subject correlation of EE and ED periods, inferred from fluctuations in subjective emotional intensity annotations across the three movie clips (negative clips from Study 1 and 2 and neutral clip from Study 1).

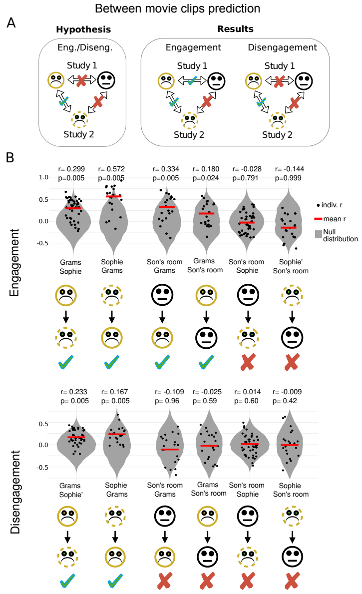

Figure 2. Illustration of criteria for assessing the generalizability of neural mechanisms underlying the EE and ED group dynamics index. (A) Schematic representation of the conditions for inferring generalizability in neural mechanisms underlying the EE and ED group dynamics index across emotionally intense movie clips. DynFC patterns trained to predict the EE and ED group dynamics index in one negative movie clip (Study 1) must be (1) successful in predicting the EE and ED group dynamics index in the other negative movie clip (Study 2), implying both independence from idiosyncratic features of the participant group and narratives, *and* (2) fail for predictions between any of the emotional narratives and the neutral narrative, implying some specificity to highly emotional contexts. (B) Results: Conditions (1) and (2) were only met for ED, where for condition (1) there was successful prediction, but for EE, only condition (1) was fulfilled, while condition (2) failed. The black dots represent Pearson's correlations between predicted and observed EE (top) or ED (bottom) based on each participant's dynFC features. Horizontal lines indicate the prediction quality reflected in the mean r across cross-validation folds. Violin plots illustrate the null distributions of mean prediction performance of models predicting the EE and ED group dynamics index after phase-randomization. The significance of empirical r was computed based on the null distribution (one-tailed tests). *DynFC*, Dynamic Functional Connectivity, *EE*, Emotional Engagement, *ED*, Emotional Disengagement.

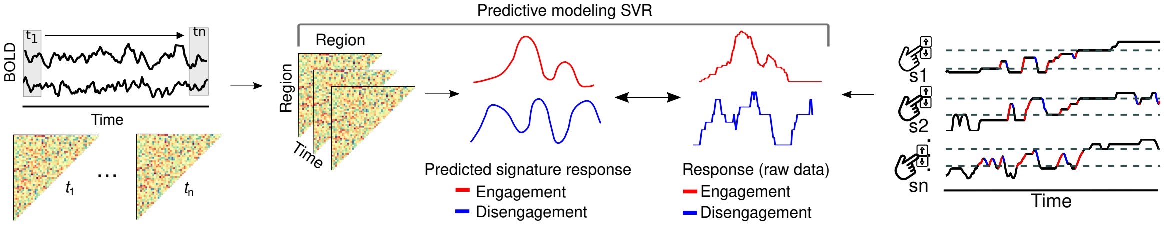

Figure 3. DynFC and Emotional Dynamics Index for EE and ED. (A) DynFC and the Emotional Dynamics Index were calculated using a sliding window approach. DynFC represents the Pearson correlation of BOLD time courses within a window (left), while the Emotional Dynamics Index for EE and ED captures the frequency of EE and ED episodes across all participants for each window. An EE and ED phase was determined by positive or negative shifts within a subject's continuous subjective emotional intensity annotations, within predefined intra-individual thresholds (right). see . *DynFC*, Dynamic Functional Connectivity, *EE*, Emotional Engagement, *ED*, Emotional Disengagement.

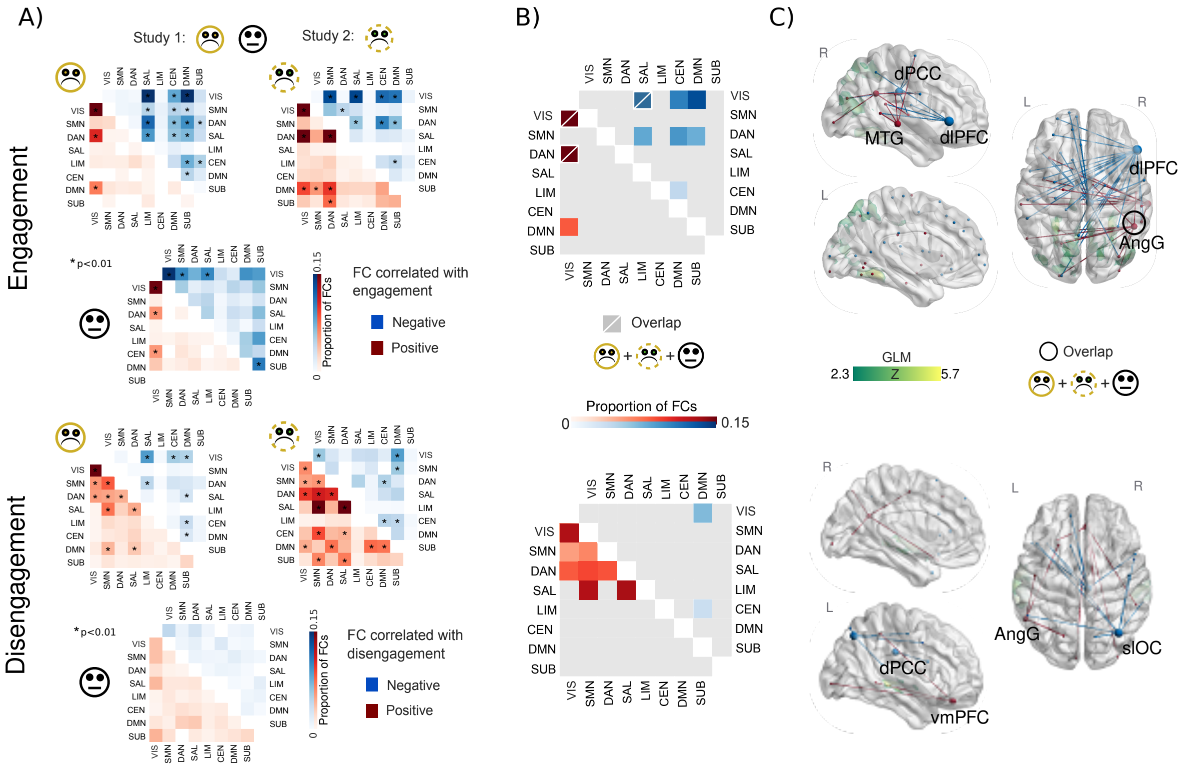

Figure 4. DynFC predicts an Emotional Dynamics Index. (A) Within each cross-validation fold, dynFCs were grouped into predefined canonical functional networks (Schaefer et al., 2018). The lower triangle matrix (red) illustrates the proportion of FCs positively correlated with the Emotional Dynamics Index for EE or ED, and the upper triangle matrix (blue) illustrates the proportion of FCs negatively correlated with the Emotional Dynamics Index for EE or ED, respectively. Asterisks indicate network pairs selected above chance (one-tailed tests, FDR-P < 0.001). The intensity of colors indicates the proportion of selected FCs from all possible network-to-network connections. (B) Shared significant FCs across negative movie clips. The crossed gray square indicates FCs shared among negative movie clips that also overlapped with the neutral clip. (C) Top two highest connected nodes in the predictive model. FCs overlapping across all three movie clips are indicated by black circles, whereas those specific to negative clips do not show black circles. *DynFC*, Dynamic Functional Connectivity, *EE*, Emotional Engagement, *ED*, Emotional Disengagement.

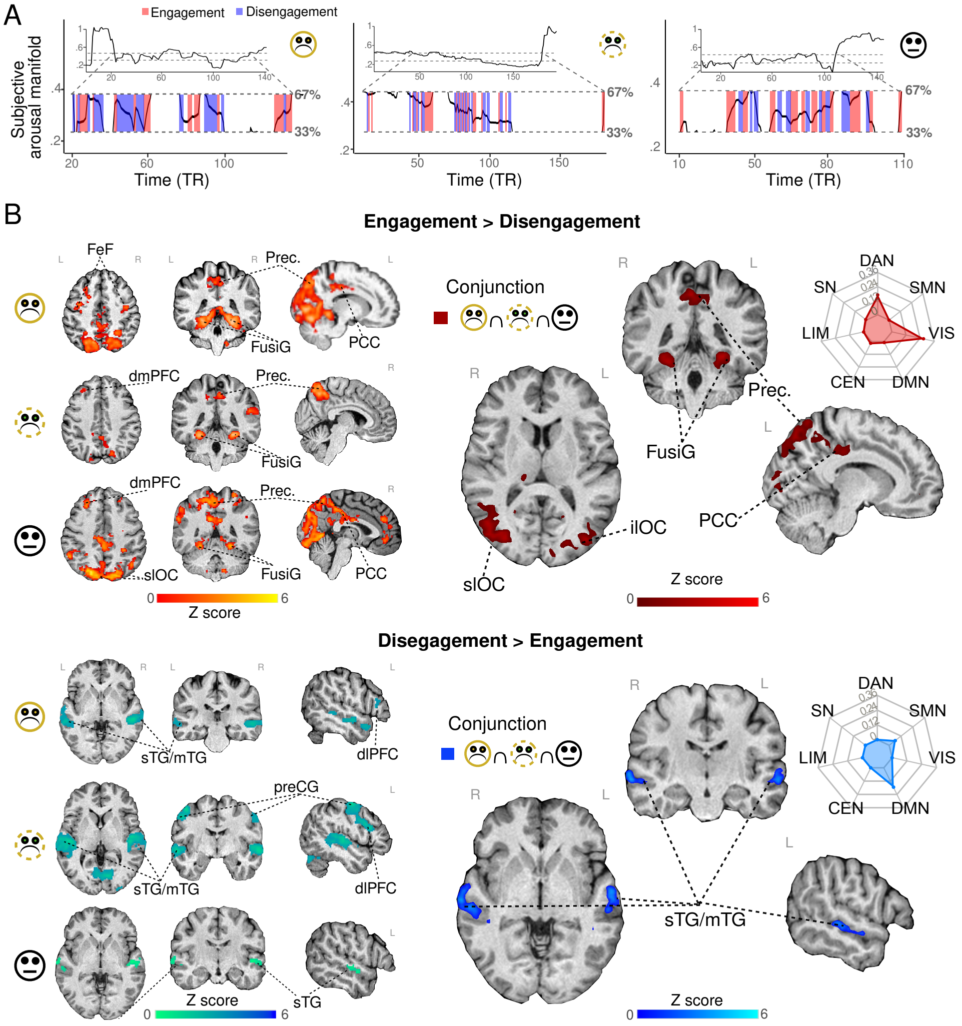

Figure 5. Group BOLD Signal Intensity is distinctively associated with lower dimensional features of group EE and ED during movie viewing. (A) Group manifold of subjective emotional intensity annotations for each movie clip represented as the time course of the first principal component. Time points of EE are marked in red, time points of ED are marked in blue. EE and ED are derived from positive and negative shifts within the group manifold (Dessu et al. (2020), see methods section). (B, left column) Thresholded (Z > 2.3) and cluster-corrected contrast images for the contrasts EE>ED and ED>EE. (B, right column) Conjunction analysis results (Nichols et al., 2005) across movie clips. Radar plots illustrate the spatial correlation strength between significant voxels of the conjunction and canonical networks (Yeo et al., 2011). *EE*, Emotional Engagement, *ED*, Emotional Disengagement, *FeF*, Frontal Eye Field, *Prec.*, Precuneus, *FusiG*, Fusiform Gyrus, *PCC*, Posterior Cingulate Cortex, *dmPFC*, Dorsomedial Prefrontal Cortex , *slOC*, Superior Lateral Occipital Cortex, *sTG/mTG*, Superior Temporal Gyrus/Middle Temporal Gyrus, *preCG*, Precentral Gyrus, and *dlPFC*, Dorsolateral Prefrontal Cortex.